Specific heat and resistivity near the charge-density-wave phase transitions in $2H$-$TaSe_2$ and $2H$-TaS_2‡

R. A. Craven†
IBM Thomas J. Watson Research Center, Yorktown Heights, New York 10598

S. F. Meyer*
Department of Physics and Materials Research Center, University of Illinois, Urbana, Illinois 61801
(Received 10 June 1977)

Detailed measurements of the specific heat and resistivity have been made on samples of $2H$-$TaSe_2$ and $2H$-TaS_2 near their charge-density-wave phase transitions. Because the crystal quality of $2H$-$TaSe_2$ is much better than that of $2H$-TaS_2, we emphasize the results on $2H$-$TaSe_2$ and make quantitative comparison with the theory of charge-density waves in this material. In $2H$-$TaSe_2$ the normal to incommensurate phase transition was found to be second order; the incommensurate to commensurate transition was first order. Specific-heat measurements on this material indicate that the zero-temperature coherence length is relatively short; $\pi\xi_0 \simeq 14$ Å. The resistivity of $2H$-$TaSe_2$ immediately above the normal to incommensurate phase transition is dominated by resistive scattering from the periodic structural deformations accompanying the charge-density waves. The specific-heat and resistivity measurements both indicate that the normal to incommensurate phase transition in $2H$-$TaSe_2$ can be analyzed within a nearly-mean-field model.

I. INTRODUCTION

In the past several years, transition metal dichalcogenides have been the focal point for a considerable amount of research effort.[1] This interest has been generated by the unique physical properties of these solids which have such a highly anisotropic layered structure. The basic building block of these crystals resembles a sandwich with a layer of transition-metal atoms between two layers of chalcogen atoms. The sandwich layer is hexagonal with the transition metal sitting in a site of either octahedral or trigonal prismatic coordination with respect to its nearest-neighbor chalcogen atoms. These two basic layer morphologies can be combined in several ways to form different polymorphs of a given transition-metal dichalcogenide. The simplest polymorph ($1T$) has octahedral coordination of the transition-metal atoms within the layer which is repeated perpendicular to the layer. A slightly more complicated structure with a larger unit cell ($2H$) has two layers of chalcogen–transition-metal–chalcogen atoms with trigonal prismatic coordination and alternate stacking perpendicular to the planes (i.e., *AcA BcB*). Because of the layered structure and bonding of the metallic dichalcogenides the Fermi surfaces of these materials are very anisotropic.[2] Couplings between the conduction electrons on these anisotropic Fermi surfaces and the lattice phonons are responsible for the nonuniform charge-density waves (CDW) and the low-temperature periodic structural deformations (PSD), which have recently been observed.[1] The stability and structure of these charge-density-wave states depends upon the shape of the Fermi surface which is in turn related to the symmetry of the polymorph under consideration.

In $1T$-$TaSe_2$, electron-diffraction experiments at high temperatures[1,3] give an undistorted hexagonal diffraction pattern which comes from the basic lattice. Below $T_0 \simeq 600$ K, new spots appear which have the same hexagonal symmetry but a different wave vector. These spots arise from the incommensurate charge-density wave.[4] At $T_d \simeq 473$ K this superlattice rotates and q_0 shrinks enabling the PSD-CDW to lock into a 3×1 commensurate state. The phase changes in the $1T$ state are first order in nature, i.e., there is a significant hysteresis and difference in free energy between the normal, undistorted state and the incommensurate CDW state and between the incommensurate CDW state (ICDW) and the commensurate charge density wave state (CCDW). In the $1T$ materials the Fermi surface is essentially flat in the k_z direction and forms open parabolic surfaces in the k_x-k_y plane symmetrically around the ΓM line.

In $2H$-$TaSe_2$, however, electron[1,3] and neutron[5] diffraction experiments indicate that there is no superlattice above $T_0 \simeq 120$ K. Below this a superlattice appears which has hexagonal symmetry and wave vector $q_a = \frac{1}{3}(1-\delta)a_0^*$, with the discommensuration parameter $\delta \simeq 0.02$. This incommensurate state is stable in most crystals down to $T_d \simeq 90$ K. At this temperature, δ, which has been decreasing with temperature, drops discontinuously to zero and a CCDW phase with $q_a = \frac{1}{3}a_0^*$ is stable. In $2H$-$TaSe_2$ the phase transition between the normal undistorted phase of the material and the ICDW phase is apparently second order; the transition

between the ICDW and CCDW is first order. In the $2H$ polymorph, the Fermi surface remains essentially flat in the k_z direction, but becomes multiply connected in the k_x-k_y plane. There is an hexagonal electron surface centered around Γ and there are smaller triangular hole pockets centered at the six K points of the Brillouin zone.

In the $1T$ polymorphs the CDW-PSD occur with a given wave vector because there is significant nesting of the Fermi surfaces, i.e., a single wave vector can span large areas of the nearly parallel sheets of the Fermi surface. The reduction in electronic energy due to the opening of the gap in the Fermi surface is sufficient to overcome the gain in elastic energy necessary to form the distortions and the PSD-CDW becomes a stable ground state. The origin of the PSD-CDW state in the $2H$ polymorph is less clear, however. Rice and Scott[6] have proposed that it is not nesting of the Fermi surfaces which is responsible for the CDW instability in $2H$-$TaSe_2$ but that it is the possibility of connecting saddle points in the band structure, which have sufficiently high density of states with a wave vector $\frac{2}{3}a_0^*$ in length. This distortion would remove the saddle point and lower the resistivity below the phase transition. McMillan[7] has developed an alternate theory. He assumes a nesting wave vector $\frac{1}{3}a_0^*$ which connects hole surfaces near the K point in the Brillouin zone and develops a microscopic model of the CDW-PSD at zero temperature. The more important impact of his theory, however, is its challenge to the conventional model which maintains that the major contribution to the entropy at finite temperatures comes from the excitation of electrons across the gap in the band structure which has been induced by the CDW. His finite temperature theory is based upon an assumption that the coherence length of the CDW state is very short and it implies that lattice entropy, not the electronic entropy, is dominant.

In the present paper we present precision measurements of the specific heat and resistivity of samples of $2H$-$TaSe_2$ and $2H$-TaS_2 in the vicinity of their second order normal to ICDW phase transitions and near the first-order ICDW to CCDW phase transition in $2H$-$TaSe_2$. An analysis of the specific-heat data is performed which reflects the presence of fluctuations for T near T_0 in $2H$-$TaSe_2$. The results of our analysis indicate that a short zero-temperature coherence length of the charge-density-wave fluctuations is consistent with the specific heat data. This result is favorably compared with recent theoretical predictions of McMillan. The resistivity of $2H$-$TaSe_2$ immediately above the normal to ICDW transition at T_0 is dominated by resistive scattering from the periodic structural deformations accompanying the charge-density waves.

In our analysis of the fluctuations effects on the specific heat and resistivity near T_0 we have found asymptotic values of the power-law exponents that would be expected if the Gaussian model[8] extension of mean field theory were valid in this material.

This paper is organized with experimental methods and results presented in Sec. II. Analysis of the specific-heat data and a comparison of our results with recent theories of CDW phase transitions is given in Sec. III. Analysis and discussion of the resistivity behavior near T_0 with a comparison of the effect of fluctuations on the specific heat and resistivity is presented in Sec. IV. A summary of our results is given in Sec. V.

II. EXPERIMENTAL RESULTS

The $2H$-$TaSe_2$ samples were prepared from 99.995% pure Ta wire and 99.999% pure Se shot. The iodine vapor transport[9] was set up at 730–640 °C and increased slowly to 760–690 °C after two days. The oven was turned off after five days. This procedure resulted in complete transport and yielded a small quantity of large, thick crystals.

Powder pattern x-ray diffraction verified the $2H$ structure and showed unusually sharp lines for these layered materials. Mass spectrographic analysis found of order 100 ppm total impurities, with calcium the largest single impurity at 40 ppm. Iron and niobium were each less than 10 ppm. One possible disorder effect remaining in the $2H$-$TaSe_2$ crystals is the presence of five common isotopes of selenium, with an 8% spread in isotopic mass.

The $2H$-TaS_2 samples were prepared from Ta wire and 99.999% pure S powder. They were iodine vapor transported from 900 to 800 °C in the $1T$ phase. Transformation to the $2H$ phase was accomplished by annealing them at 600 and 500 °C for two days each. Because the unit cell experiences a volume change at the $1T$-$2H$ phase transformation, the crystals are wrinkled and experience a large internal strain. As a result, the x-ray diffraction spectrum of $2H$-TaS_2 has linewidths which are 50% broader than those in the $2H$-$TaSe_2$ spectrum. One expects this strain in TaS_2 to lead to broadening of the superconducting and CDW transitions. The $2H$-$TaSe_2$ crystals have no such effect and therefore should give sharper transitions.

Specific heat measurements on the layered samples were made using an ac calorimeter.[10] The heat pulse to the sample was provided by interrupting the light from a tungsten-halogen light with a

mechanical chopper. Details of the experimental method and apparatus have been published previously.[11] The proper operating conditions are those where the internal thermal relaxation time of the sample-thermometer combination τ_1 and the relaxation time between this sample thermometer and the dc background, τ_2, obey the relationship $\tau \ll 1/\omega \ll \tau_2$. When this is satisfied the temperature excursions of the sample are inversely proportional to the operating frequency. Results for the frequency dependence of the temperature excursions of a sample of $2H$-$TaSe_2$ are shown in Fig. 1. The specific-heat measurement on this sample was taken at 14.2 Hz. Measurement of the absolute temperature and ac temperature excursions were made with cromel-alumel thermocouples.

The ac specific heat method used gives high-precision relative measurements, but does not give absolute measurements of the specific heat without detailed knowledge of the power absorbed from the light pulse. Absolute measurements were performed in a separate calorimeter using a thermal relaxation method and joule heating. The absolute results were, to within our experimental error (±6%), equal to the values reported by Harper,[12] and, since his reported error for the absolute value is smaller (±3%), we have used his absolute values to calibrate our relative ac measurements. Our specific-heat measurements far from the transition regions agree with his absolute data.

The specific-heat results on one sample of $2H$-$TaSe_2$ extending from 80 to 140 K illustrate the overall features of interest. (Fig. 2). The normal to ICDW phase transition occurs at 120.6 K and indicates the presence and importance of fluctuations but gives no indication of hysteresis.

The incommensurate charge-density-wave to commensurate charge-density-wave phase transition in this sample takes place near 110 K. This phase transition is indicated by a small nearly discontinuous rise in the specific heat when the temperature of the sample is increased so that the sample goes from the CCDW phase to the ICDW phase and a similar nearly discontinuous drop in the specific heat when the sample temperature is decreased and the sample goes from the ICDW to the CCDW phase. There is a different transition temperature which is dependent on the rate and direction of the temperature change. This hysteresis gives strong additional evidence that this ICDW to CCDW phase transition is first order. The specific heat immediately above the small discontinuity is about 0.4 J/mol K larger than the specific heat just below the discontinuity. This is not a measure of the latent heat, however, since the ac technique is not very sensitive to latent heat

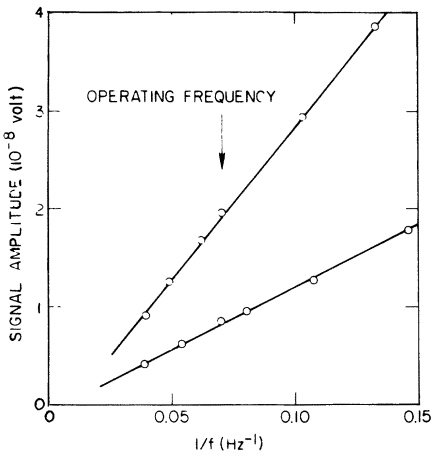

FIG. 1. Sample response as a function of frequency. Linear relationship implies $1/\tau_1 \ll \omega \ll 1/\tau_2$, and that $C_p \propto (\Delta T)^{-1}$.

singularities which occur at first-order phase transitions. In these circumstances,[13] the latent heat affects only a few cycles (less than or approximately equal to the time constant of the lock-in) of the temperature oscillations of the sample and does not appear as a spike in the specific-heat data. The jump in specific heat does represent the difference in the specific-heat values on either side of the transitions. The ICDW-CCDW transition temperature in this sample is the highest that has been seen for this material.

The hysteresis loop and differences in the specific heat between the ICDW and the CCDW are larger for this sample than for other samples from this batch of material which have this phase

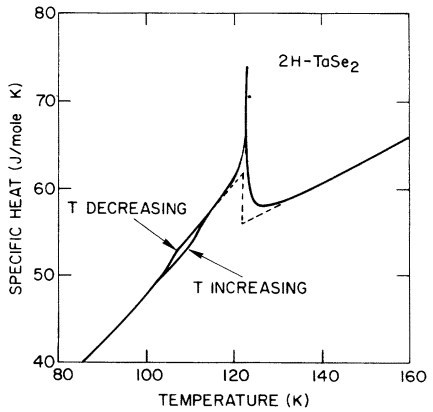

FIG. 2. Specific heat of $2H$-$TaSe_2$ near the normal to ICDW transition at 120.6K and the ICDW to CCDW phase transition at $\simeq$110 K. The dashed line near the normal to ICDW phase transition (at T_0) indicates an estimate of mean-field behavior near T_0. Hysteresis at the lower (ICDW-CCDW) implies that this transition is first order.

transition at a lower temperature. Most of our samples had phase transitions between 90 and 98 K. The larger hysteresis loop associated with the higher transition temperature is consistent with the larger value of the discommensuration parameter, δ, which is expected to exist at this temperature,[5] and with the presumed larger free-energy difference between the ICDW and CCDW ground state which is associated with this δ.

The second-order phase transition between the normal state and the uncommensurate charge-density wave state at 120.6 K has a large specific-heat anomaly associated with it. We can calculate a lower bound for the energy involved in this phase transition by fitting a mean field model to the data near T_0 (normal to the ICDW transition). As we have illustrated by the dashed line in Fig. 2, the mean-field estimate is made by extrapolating the nearly linear specific-heat curve for temperatures far from T_0 (reduced temperature $|t| \equiv |(T - T_0)/T_0| \geq 0.1$) into the phase transition temperature. The difference in the specific heat above and below the transition which is estimated by these straight lines extrapolations is $\simeq 4$ J/mol K.

We can see in Fig. 2 that there is clearly an excess of specific heat above this straight line approximation. This excess specific heat is due to fluctuation effects in the vicinity of this second-order phase transition and the exact power-law dependence of these results will be determined in Sec. III. The point-by-point data which will be analyzed in Sec. III is shown in Fig. 3. We have calculated the excess enthalpy under this specific-heat curve by fitting a smooth background through the data far from T_0. This approximation is similar to what Harper has done with data taken by a scanning calorimeter. Our estimate of the enthalpy of 67 J/mol is close to his value 55 J/mol and within his experimental accuracy. This gives additional confirmation that there is no excess latent heat associated with a first-order transition at T_0.

Measurements of the specific heat of $2H$-TaS_2 are shown in Fig. 4. The absolute calibration of these data was done in a separate calorimeter using a thermal-relaxation method. The sample used for calibration purposes weighed 149.12 mg and came from the same growth batch as the sample which was measured in the ac calorimeter. The absolute specific heat was measured from 30 to 100 K and the temperature dependence agreed with the ac data to within our error bars ($\pm 10\%$).

The severe sample strain in $2H$-TaS_2 which was mentioned above is probably responsible for the rounding of the specific heat in the vicinity of the phase transition. We do not see any evidence of hysteresis,[14] however, and cannot tell from our measurements when the ICDW-CCDW transition is taking place. Predictions that this lock-in transition can be lowered by the presence of impurities should also apply to strain. The ICDW-CCDW transition might be completely suppressed for this material.

We have indicated by the dashed line in Fig. 4 an extrapolation of the nearly linear specific-heat curve far from the transition. This mean-field-approximation gives us a lower bound for the energy involved in the charge-density-wave transition in $2H$-TaS_2. A jump in the specific heat of 2.8 J/mol K is indicated by this extrapolation. Even in the presence of rounding caused by strains, the specific heat at T_0 seems to be diverging faster than the mean-field approximation for this material. Although we have not done a detailed analysis of the power-law behavior of the specific heat of $2H$-TaS_2 because the material is

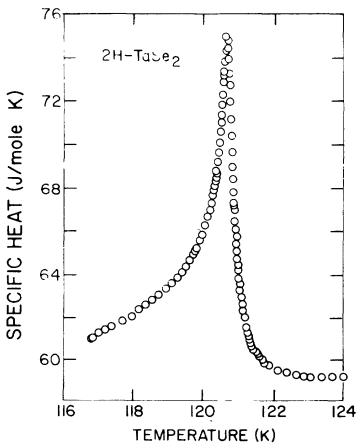

FIG. 3. Detail of specific heat near normal to ICDW phase transition for $2H$-$TaSe_2$.

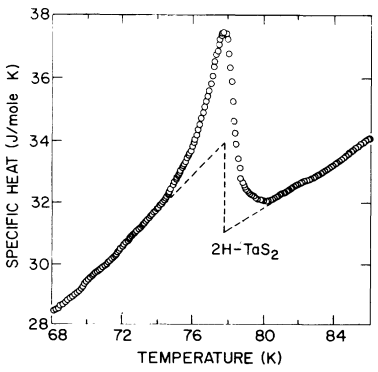

FIG. 4. Specific heat at charge-density wave transition for $2H$-TaS_2. No hysteresis was observed or ICDW-CCDW transition detected. The dashed line is an estimate of mean-field behavior in this system.

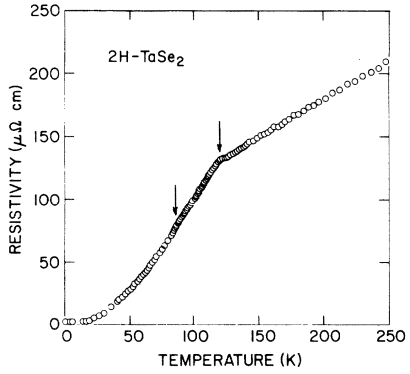

FIG. 5. Resistivity of $2H$-$TaSe_2$ as a function of temperature. Anomalies at normal to ICDW and ICDW to CCDW phase transitions are visible and noted by arrows.

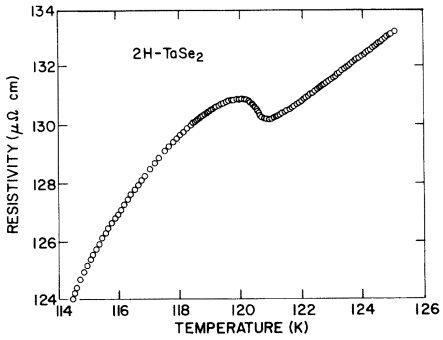

FIG. 6. Details of the resistivity near the normal to ICDW phase transition in $2H$-$TaSe_2$. The phase transition is at the point of maximum negative slope.

strained, we feel that a positive exponent would not be inconsistent with this data.

Resistivity measurements along an a axis of $2H$-$TaSe_2$ and $2H$-TaS_2 have also been made by a four-probe dc method from 4 to 300 K. The results for one sample of $2H$-$TaSe_2$ are shown in Fig. 5. The resistivity is essentially linear from room temperature down to the vicinity of the normal to ICDW phase transition. This linear resistivity intercepts zero temperature at a value much higher than expected for a normal metal. As the phase transition is approached from above, the resistivity starts to increase, with the slope dR/dT reaching a maximum negative value at T_0. Below T_0 the resistivity goes through a maximum then decreases monotonically to its measured normal state value at $\simeq 4$ K. Kinks in the R vs T curve, which have been seen before at T_d,[15] are indicated by arrows on the figure. The resistance ratio for the samples measured was very high, ranging from 200 to 400. There was no correlation, however, between the higher resistance ratio and higher T_d. Variations of T_d between 90 and 110 K from sample to sample are not yet well understood.

The temperature dependence of the resistivity near T_0 has been examined in greater detail using two different methods. First of all, we used an ac Wheatstone bridge with a lock-in amplifier as a null detector to measure the resistivity with greater precision (1 part in 10^5). These results are shown in Fig. 6. The resistivity is smooth and shows no hysteresis near T_0. The temperature derivative of the resistivity near T_0 was also measured using a thermal modulation technique.

In this later technique,[16] a constant dc bias current is passed through the sample at the same time that a small, spatially uniform thermal modulation is applied. The small change in temperature changes the resistivity, and hence the voltage drop across the sample. In the limit of small temperature oscillations compared to the dc temperature drift we find that

$$\frac{1}{R}\frac{dR}{dT} = \frac{1}{V}\frac{\Delta V}{\Delta T}.$$

The thermally modulated resistivity derivative and the specific heat of the sample were measured simultaneously. This is advantageous since it clearly defines the relationship of the resistivity derivative to the phase transition. Our results for $2H$-$TaSe_2$ clearly indicate that the phase transition at T_0 which we see in the specific heat coincides with the negative singularity in the temperature derivative of the resistivity. Since we modulated the temperature of our sample with a chopped light pulse of constant power, simultaneous measurement of the voltage oscillations and the temperature oscillations which are related to the inverse of the specific heat is necessary. The temperature oscillations change dramatically near T_0 for a constant heating power.

The temperature derivative of the resistivity has also been measured for $2H$-TaS_2 using the thermal modulation technique. The results of these measurements are shown in Fig. 8 and they indicate that the maximum negative slope in the resistivity is at the same temperature as the maximum in the specific heat. The anomaly in the derivative of the resistivity is not as sharp in $2H$-TaS_2 as it is in $2H$-$TaSe_2$. This rounding or smearing of the resistivity is also a reflection of the strain in the crystals of $2H$-TaS_2.

The resistivity measurements of Figs. 6–8 bear remarkable similarity to the resistivity measurement on dysprosium, an anisotropic antiferromagnet.[17] In that material, a gap is opened up at the Fermi surface by a magnetic superlattice which has a wave vector Q_s near $2k_F$. The detailed temperature dependence of $(1/R)(dR/dT)$ and its relation to fluctuation in the charge-density-wave materials will be examined in Sec. IV.

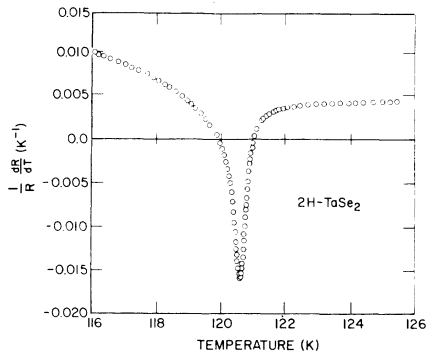

FIG. 7. Normalized temperature derivative of the resistivity for $2H$-$TaSe_2$ near the normal to ICDW phase transition. Derivative was taken by thethermal modulation technique.

III. DISCUSSION OF SPECIFIC-HEAT RESULTS

The results on the specific heat which were shown in Sec. II indicated that fluctuation effects were visible in the specific heat of $2H$-$TaSe_2$ near the second-order phase transition from the normal state to the incommensurate charge-density-wave state. In this section we analyze the critical behavior of these results and then compare our results to recent theoretical predictions for the behavior of charge-density-wave systems.

The specific heat in the vicinity of T_0 should be describable by a function of the reduced temperature $t=(T-T_0)/T_0$. For positive t this function becomes

$$C_p^+ = A^+(t^{-\alpha}-1)/\alpha + B^+ + Dt\,,$$

and for negative t,

$$C_p^- = A^-(|t|^{-\alpha'}-1)/\alpha' + B^- + Dt\,.$$

These functions describe the specific heat in terms of many parameters (A^+, A^-, B^+, B^-, α, α', D, T_0) and a blind approach to determining these parameters is extremely complicated. We have used a method of analysis similar to that used by Lederman, Salamon, and Shacklette[18] to test the universality hypothesis on various ferromagnets and antiferromagnets. Their analytical technique introduces additional physical constraints in two distinct steps and it allows a more self-consistent determination of the parameters from the data. One of the first assumptions in the above equations is that the lattice contribution to the specific heat is not singular for temperatures near T_0 and that it can be approximated by a linear term proportional to D. This assumption of linearity is not entirely correct and, as we will discuss later, a better estimate can improve the fit somewhat. Subtracting off the lattice background and defining $\tilde{C}_p^{\pm} = C_p^{\pm} - Dt$, we can compare the data above and below the transition for equal values of $|t|$ and we find

$$\tilde{C}_p^+ = \frac{A_+}{\alpha}\left[\left(\frac{(\tilde{C}_p^- - B^-)\alpha'}{A}+1\right)^{\alpha/\alpha'} - 1\right] + B^+ .$$

According to mean-field and asymptotic critical calculations there should be symmetry in the specific heat measured about T_0, that is, α should equal α'. If we set $\alpha=\alpha'$ in this equation we find that the specific heat above the transition scales linearly with the specific heat below the transition,

$$\tilde{C}_p^+ = (A^+/A^-)\tilde{C}_p^- + (B^+ - A^+B^-/A^-)\,.$$

A plot of $\tilde{C}_p^+$ vs $\tilde{C}_p^-$ for equal values of $|t|$ is shown in Fig. 9. The linearity of this plot implies $\alpha=\alpha'$. We have analyzed the data in two different ways. We first assumed that the lattice background could be approximated by a linear term. Although the

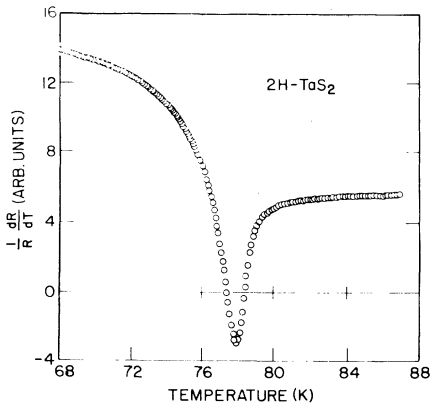

FIG. 8. Temperature derivative of the resistivity for $2H$-TaS_2 near its charge-density-wave transition.

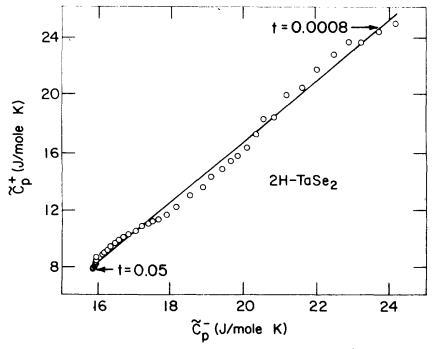

FIG. 9. Excess specific heat above the normal to ICDW phase transition as a function of the specific heat below the phase transition with temperature as an implicit variable. The linear relation implies $\alpha=\alpha'$. The extrema of $t=|(T-T_0)/T_0|$ are indicated.

fit to a straight line of $\tilde{C}_p^+$ vs $\tilde{C}_p^-$ for small values of $|t|$ was quite good, there was significant systematic variation for large values of $|t|$. An alternative approach is to calculate a reasonable lattice background based on the similarity between the $2H$-$TaSe_2$ structure and the structure of MoS_2. Neutron scattering experiments have been done for MoS_2 in order to determine the phonon dispersion curves and the phonon density of states.[19] This density of state reflects the layered natures of the crystal, the fact that the lattice vibrations in the plane are much more energetic than flexural modes perpendicular to the planes. Specific-heat calculations based on this density of states indicate a monotonically increasing and temperature-dependent Debye temperature Θ_D. We have used this $\Theta_D(T)$ normalized to $\Theta_D = 140$ K of $TaSe_2$ for low temperatures[12] to derive the lattice background shown in Fig. 10. Using this function and a small value of D improved the fit of a straight line to the data for larger $|t|$. We show this fit in Fig. 9. The transition temperature has been chosen to be 120.6 K. Variations of T_0 by 0.1 K become quite noticeable and $T_0 = 120.6$ K represents a minimum in the least-square deviation of the data from a straight line.

Once we have determined D, T_0, and the fact that $\alpha = \alpha'$ from the linear relationship between $\tilde{C}_p^+$ and $\tilde{C}_p^-$, we can merge the data below T_0 with the data above T_0. This algebraically merged data is then plotted semilogarithmically, i.e., $\tilde{C}_p^{\pm}$ vs $\log_{10}|t|$, to determine the sign of α and α'. This plot is shown in Fig. 11. A straight line on this plot would correspond to a logarithmic divergence and would imply that $\alpha = \alpha' = 0$. An upward curvature (positive second derivative) implies that the specific heat is diverging faster than logarithmic, i.e., $\alpha > 0$; a downward curvature (negative second derivative) implies that $\alpha < 0$ and that the specific heat has a cusped singularity rather than divergent singularity at T_0. It is immediately clear from inspection of Fig. 11 that $\alpha > 0$.

We have fit the function

$$\tilde{C}_p^{\pm} = (A/\alpha)(|t|^{-\alpha} - 1) + B$$

to the data minimizing the χ^2 of the deviations as a function of all three parameters A, B, and α. We include the uncertainty in the specific heat and uncertainty in our ability to determine the reduced temperature t. We find a global minimum in the χ^2 of the deviations for $\alpha = \alpha' = 0.45 \pm 0.035$, $A = 0.191 \pm 0.036$, and $B = 14.1 \pm 0.2$. The value that we find for α is extremely large compared to what one would expect from theories of asymptotic universality ($\alpha \simeq -0.01$). It is possible, however, that the transition can be described by the Gaussian approximation, a lowest-order extension of

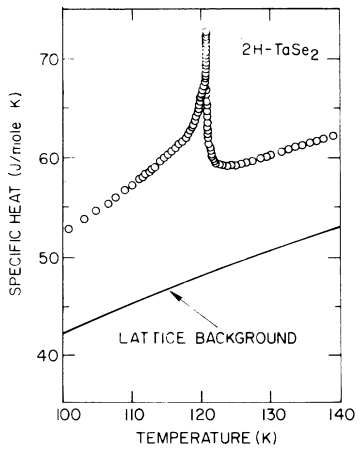

FIG. 10. Lattice background specific heat used for the critical point analysis.

mean-field theory.[20] The Gaussian model predicts that the specific heat should diverge like $t^{2-d/2}$. For a system with three-dimensional fluctuations $d = 3$ and $\alpha = \alpha' = \frac{1}{2}$. One possible explanation for seeing nearly-mean-field behavior in the asymptotic critical region is that the system is in the vicinity of a tricritical point. Such a suggestion has recently been made on the basis of a model which describes the energetics of amplitude and phase variations associated with the incommensurate phase.[21]

The excess specific heat above the linear mean-field estimate shown in Fig. 2 for $T > T_0$ is a direct measure of the scale of fluctuations when the Gaussian approximation is valid. In this region $C_p^+\sqrt{t} = (2\pi\xi_0)^{-3}$ where ξ_0, the zero-temperature coherence length, is a measure of the scale of fluctuations.[20] From the specific-heat data above T_0 we find $C_p^+\sqrt{t} \cong 0.8$ J/mol K or $\pi\xi_0 \cong 14$ Å. This number represents a spherical average coherence

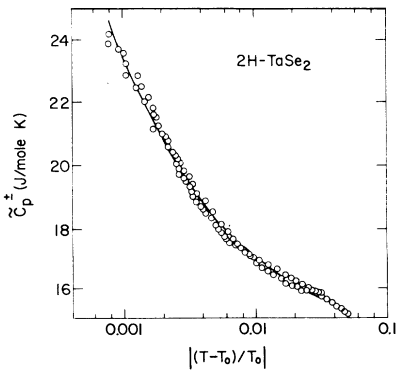

FIG. 11. Excess specific heat (merged data from above and below T_0) as a function of $\log_{10}|(T - T_0)/T_0|$. Curve represents a least-square fit $\alpha = \alpha' = 0.45 \pm 0.035$.

length for $2H$-$TaSe_2$; $\xi_0 = (\xi_{\parallel a}, \xi_{\perp a}, \xi_c)^{1/3}$.[5]

We can also use the specific results on $2H$-$TaSe_2$ presented in Sec. II to make a quantitative comparison between the predictions of a conventional theory of charge-density-wave transitions and McMillan's recent model for $2H$-$TaSe_2$. The former theory assumes there is a long coherence length ξ_0 and that the major contribution to the entropy at temperature $T>0$ comes from electronic excitations. McMillan's model, however, is based upon a short coherence length and concludes that phonon entropy is very important near the normal to ICDW phase transitions.

The conventional model, derived by Chan and Heine,[22] is a mean-field model (for large ξ_0, fluctuations are negligible). They find a gap equation which is similar to the BCS gap equation for a superconductor. Using BCS, then, a transition temperature can be found,

$$k_B T_0 = 1.13 E_B \exp[-N_a A/2g^2 N_\uparrow(0)] \quad (1)$$

where E_B is the bandwidth, N_a the density of Tantalum atoms, A the bare elastic constant, g the electron-phonon coupling parameter, and $N_\uparrow(0)$ the density of states at the gap for a given spin state for each CDW. The energy gap at $T=0$ becomes

$$2W(T=0) = 3.52 k_B T_0; \quad (2)$$

the heat capacity jump at T_0 (mean field) is for a 3 CDW state,

$$\Delta C_v = 3 \times 9.4 N_\uparrow(0) k_B^2 T_0; \quad (3)$$

and the change in susceptibility due to the opening of the band gap is

$$\Delta\chi = \chi(T_0) - \chi(0) = 5.2 \mu_B^2 N_\uparrow(0). \quad (4)$$

In order to compare this model with the specific-heat experiment, we use the susceptibility measurements[3] to find $\Delta\chi = 55 \times 10^{-6}$ emu/mol. Using Eq. (4) we find $N_\uparrow(0) = 0.33$ (state/eV Ta-atom). This model then predicts $\Delta C_v = 0.8$ J/mol K from Eq. (3). Our specific-heat results are clearly in contradiction with this model. First of all, we do see evidence of fluctuations; secondly, if we estimate the size of the mean-field jump by extrapolating the nearly linear portion far from T_0 we find $\Delta C_p \simeq 4$ J/mol K. This is five times larger than the predictions of the conventional theory.

McMillan has developed a finite temperature theory based on a short coherence length. When the coherence length is small, phonon frequencies (k_c cutoff $\simeq 1/\xi_0$) are modified over a large region of reciprocal space near the CDW wave vector. This lowers the normal to ICDW phase transition from what it would be if a large number of phonons were not involved, and leads to a prediction that the zero-temperature gap is $\gg 3.5\, kT_0$. Using the elastic parameters for the phonon frequencies which were determined from the low-temperature Raman data of Holy, *et al.*,[23] and the transition temperature T_0, an estimate of the specific-heat jump of 1.67 k_B/mode can be made.[7] The measured specific-heat jump is 4 J/mol K = 0.48 k_B/Ta-atom. This implies that there are 3 modes per 10 Ta atoms, or that the correlated area is about equal to the superlattice cell area. The coherence length becomes $\pi\xi_0 \simeq 10$ Å, which is as short as is physically reasonable. McMillan points out that this seems to be in agreement with other measurements, particularly neutron scattering results and the weak absorption edge in the infrared reflectivity at 0.25 eV.[24] This is also in remarkably good agreement with the zero-temperature coherence length which we found earlier in this section from analysis of the excess specific heat above T_0, $\pi\xi_0 \cong 14$ Å. The two estimates both indicate that a short coherence-length model is very reasonable for $2H$-$TaSe_2$.

IV. DISCUSSION OF THE RESISTIVITY FOR T NEAR T_0

The detailed analysis of the specific-heat results has indicated that fluctuation effects near T_0, the normal state to incommensurate state phase transition, can be described by a three-dimensional nearly-mean-field model. We have analyzed the temperature dependence of the resistivity near T_0 in order to give additional evidence for these fluctuations, and to test the applicability to $2H$-$TaSe_2$ of general theories of the electrical resistivity near second-order phase transitions.

Most of these theories originated from the study of the resistivity of a metal near a magnetic phase transition, but they can be applied to more general problems. Some landmark papers in this field are those of de Gennes and Friedel,[25] who suggested that the temperature dependence of the spin-spin correlation function should be important to the critical scattering of electrons near a ferromagnetic phase transition; Fisher and Langer,[26] who used a more complete knowledge of the wave vector and asymptotic temperature dependence of the spin-spin correlation function to predict that the temperature derivative of the resistivity near a ferromagnetic transition should look like the specific heat; and Suezaki and Mori,[27] who looked in greater detail at the electrical resistivity near an antiferromagnetic transition and predicted that because of large angle scattering and the divergence in the spin-spin correlation function at value of Q near $2k_F$, the temperature derivative of the resistivity should have a strong negative divergence. In all of these theoretical treatments there is one important and

underlying assumption; that in metals the electrical resistivity samples only the static and not the dynamic properties of the critical fluctuations. This is true for two reasons, (i) elastic scattering processes dominate the electrical resistivity in a metal and (ii) the conduction electron passes through the spatially restricted region of a critical fluctuation in a time which is short compared to the lifetime of this fluctuation. As the transition is asymptotically approached, the latter assumption remains valid because the lifetime of the fluctuations increase, that is, there is "critical slowing down."

The phase transition in $2H$-$TaSe_2$ between the normal state and the incommensurate charge-density-wave state is not a magnetic phase transition, but there are many similarities between this phase transition and the antiferromagnetic phase transition.[28] Above T_0, the normal to incommensurate charge-density-wave transition, there are fluctuations involving periodic structural deformations. These structural deformations provide a periodic potential which corresponds to twice the Fermi wave vector in the solid. An electron will be strongly scattered by this potential and suffer a large change in momentum. Electronic scattering from these structural deformations will be resistive.

One major difference between the rare earth antiferromagnets and the layered dichalcogenide with charge-density waves is that the CDW's and PSD's in the layered materials are driven by the electron-phonon interaction between the conductor electrons and the underlying lattice, whereas the magnetic moments which are scattering the electrons in rare earths are intrinsic to its atomic electronic configuration. Because of this, a complete discussion of the resistivity in a layered material must take into account the many-body nature of the interaction and include this fully renormalized electronic susceptability. We do not feel, however, that such a treatment is necessary to understand the temperature dependence of the resistivity for temperatures near T_0. As stated above, such resistivity is dominated by elastic processes with quasi-static fluctuations. Horn and Guidotti[29] have recently published an analysis of the resistivity near the Peierls transition in anisotropic conductors. The results that they derive for a three-dimensional material with large anistropy in the conductivity is applicable to the phase transition between the normal state and the ICDW state in $2H$-$TaSe_2$.

In $2H$-$TaSe_2$ the population of the fluctuating periodic structural deformations is related to the dynamical structure factor $S(k, \omega)$. The temperature dependence of the resistivity for T near T_0 is dominated by the behavior of $S(k, \omega)$ for $\omega \simeq 0$ and $k = 2k_F$. Horn and Guidotti[26] find that for $T > T_0$,

$$\frac{d\rho}{dT} \cong \frac{(2k_F)^2}{|2k_F|} |g_{2k_F}| kT \int \frac{dS(k', 0)}{dT} d^2k'$$

when g_{2k_F} is the magnitude of the electron-phonon coupling parameter and the integration is over the two dimensions since the initial and final states are strongly restricted to the basal plane of the CDW system ($\rho_{\parallel}/\rho_{\perp} \cong 30$). Although the scattering is two dimensional, the fluctuations of the PSD are three dimensional in nature.[30,31] Using the known three-dimensional dependence of $S(k, 0)$,[32] we find $d\rho/dT \simeq t^{-(1+\eta)}$. When the sample is still in the mean-field region, the temperature derivative of the resistivity should go like $d\rho/dT \simeq t^{-1}$, since $\eta = 0$. For temperatures in the asymptotic critical region the divergence should be stronger since $\eta \neq 0$, but is equal to a small positive number.

A logarithmic plot of the temperature derivative of the resistivity for $2H$-$TaSe_2$, $(1/R) \times (dR/dT)$ vs $\log_{10}(t)$ is shown in Fig. 12. Far from the transition temperature the resistivity is not dominated by the divergent fluctuations associated with the charge-density wave, and the logarithmic derivative of the resistivity becomes nearly constant. In order to analyze the behavior of the resistivity of $2H$-$TaSe_2$ near T_0, we have subtracted this constant background (B) determined from this behavior far from T_0. The straight line which is drawn on Fig. 12 represents a least-square fit to our data. The slope of this line equals -1.03 ± 0.1 and indicated that the resistivity $2H$-$TaSe_2$ above T_0 can be described by the model of Horn and Guidotti. Since $\eta \cong 0$ even for non-mean-field behavior it is difficult to determine from these results the exact size of the asymptotic critical region, however.

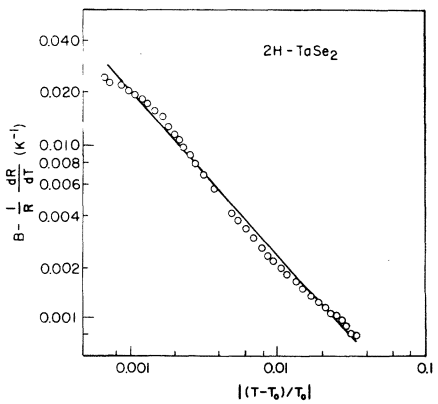

FIG. 12. Log of the resistivity derivative versus reduced temperature. Straight line is a least-square fit of slope -1.03 ± 0.1.

If the logarithmic temperature derivative of the resistivity goes like T^{-1}, one would expect that at T_0 the resistivity itself would actually diverge. Since this does not happen, one must conclude that at some temperature very close to T_0 the theory should not be applicable. In the magnetic case, Kasuya and Kondo[33] argue that sufficiently close to T_0 the singularity should behave like $(1/\rho)(d\rho/dT) \simeq t^{\alpha}$, and hence the resistivity should not diverge. A similar result which is based on the behavior of the dynamical structure factor at all wave vectors must also hold true for this charge-density-wave transition.

For temperatures less than T_0, analysis of the resistivity becomes more difficult. Fluctuations in $S(k, \omega)$ are still important to the scattering, but the density of electronic states available for conduction is also being lowered due to the opening of the Peierls gap. This change in the effective number of carriers should be related to $|t|^{\beta}$ where $\beta = \frac{1}{2}$ for a mean-field model. A calculation including the importance of both of these terms for $T < T_0$ in the layered materials has not been done. Analysis of the data for $T < T_0$ indicates $(1/R)(dR/dT) \simeq |t|^{0.3}$, which is not in agreement with these simple predictions.

V. SUMMARY

We have presented detailed measurements of the specific heat and resistivity of $2H$-$TaSe_2$ and $2H$-TaS_2 in the vicinity of the charge-density-wave phase transitions. The major emphasis has been on $2H$-$TaSe_2$ where we have shown that the size of the specific heat anomaly and the precursive fluctuations above the phase transition indicate a short coherence length $\pi\xi_0 = 14$ Å. This short coherence length is consistent with McMillan's model for these phase transitions, with the electronic contribution to the entropy at high temperature being dominated by the phonon contributions. The normal to incommensurate phase transition is second order, the incommensurate to commensurate phase transition is first order and sample dependent. A critical exponent analysis of the specific heat gives $\alpha = \alpha' = 0.45 \pm 0.035$ which is nearly consistent with predictions of the Gaussian approximation, an extension of mean-field theory.

Resistivity measurements indicate a negative divergence in $(1/R)(dR/dT)$ at T_0, the normal to incommensurate phase transition. The temperature dependence of the resistivity for $T > T_0$ is dominated by divergence in the dynamical structure factor and the resistivity above T_0 goes like $t^{-1.03\pm0.1}$. The fluctuations are resistive near T_0 and a gap at the Fermi surface opens up below this temperature.

Measurements on $2H$-$TaSe_2$ are in qualitative agreement with this, but the microscopic strains in these samples smear the phase transition and prevent detailed quantitative comparison.

---

‡Work at Illinois supported in part by ERDA Contract No. E(11-1)-1198.

†Present address: Monsanto Co., 800 N. Lindbergh, St. Louis, Mo. 63166.

*Present address: Lawrence Livermore Laboratory, Livermore, Calif. 94550.

[1]For recent reviews on this subject see: J. A. Wilson, F. J. DiSalvo, and S. Mahajan, Adv. Phys. 24, 117 (1975); J. A. Wilson and A. D. Yoffe, Adv. Phys. 18, 193 (1969); A. D. Yoffe, Chem. Soc. Rev. 5, 51 (1976).

[2]L. F. Mattheiss, Phys. Rev. B 8, 3719 (1973).

[3]J. A. Wilson, F. J. DiSalvo, and S. Mahajan, Phys. Rev. Lett. 32, 882 (1974).

[4]We refer to the intermediate phase as an incommensurate phase rather than a discommensurate phase for historical reasons, and do not claim to be able to distinguish between them by this choice. Incommensurate implies that the superlattice can be described by a single sine or cosine function with a wave vector which is different from any reciprocal-lattice wave vector. Discommensurate, on the other hand, assumes that anharmonic terms must be included in a description of the superlattice and implies that the distortion is actually composed of short commensurate segments which are connected by regions of phase slippage.

[5]D. E. Moncton, J. D. Axe and F. J. DiSalvo, Phys. Rev. Lett. 34, 734 (1975) and D. E. Moncton, J. D. Axe and F. J. DiSalvo (unpublished).

[6]T. M. Rice and G. K. Scott, Phys. Rev. Lett. 35, 120 (1975).

[7]W. L. McMillan, Phys. Rev. B (to be published).

[8]For a tutorial discussion see, S. K. Ma, *Modern Theory of Critical Phenomena* (Benjamin, New York, 1976).

[9]F. J. DiSalvo, G. W. Hull, L. H. Schwartz, J. M. Voorhove, J. V. Waszczak, J. Chem. Phys. 59, 1922 (1973); R. F. Gamble, J. H. Osiecki, F. J. DiSalvo, J. Chem. Phys. 55, 3525 (1971).

[10]Y. A. Kraftmaker, Zh. Prikl. Mekh. Tekh. Fiz. 5, 176 (1962).

[11]M. B. Salamon, Phys. Rev. B 2, 214 (1970); A. J. Schultz, G. D. Stucky, R. A. Craven, M. J. Schaffman, and M. B. Salamon, J. Am. Chem. Soc. 98, 5191 (1976).

[12]J. M. E. Harper, Ph.D. dissertation (Stanford University, 1975) (unpublished); J. M. E. Harper, T. H. Geballe, and F. J. DiSalvo, Phys. Rev. B 15, 2943 (1977).

[13]For a discussion of first-order effects see P. R. Garnier and M. B. Salamon, Phys. Rev. Lett. 27, 1523 (1971), and P. R. Garnier, Ph.D. dissertation (University of Illinois, 1972) (unpublished).

[14]Earlier resistivity measurements on $2H$-TaS_2 have indicated sharp structure at $T \simeq 75$ K. This was referred to as hysteresis, although traces in both tem-

perature directions were not shown. We do not see any hysteresis or evidence of latent heat, but we cannot rule this out for different samples. Because of the sample strain the presence or absence of a slightly uncommensurate phase has not been determined. See, J. P. Tidman, O. Singh, A. E. Curzon, and R. F. Frindt, Philos. Mag. 30, 1191 (1974).

[15]C. W. Chu, L. R. Testardi, F. J. DeSalvo, and D. E. Moncton, Phys. Rev. B (to be published).

[16]D. S. Simons and M. B. Salamon, Phys. Rev. Lett. 26, 750 (1971).

[17]R. A. Craven and R. D. Parks, Phys. Rev. Lett. 31, 383 (1973).

[18]F. J. Lederman, M. B. Salamon, and L. W. Shacklette, Phys. Rev. B 9, 2981 (1974).

[19]N. Wakabyashi, H. G. Smith, and R. M. Nicklow, Phys. Rev. B 12, 659 (1975).

[20]See S. K. Ma (Ref. 8), p. 96.

[21]S. A. Jackson, P. A. Lee, and T. M. Rice, Bull. Am. Phys. Soc. 22, 280 (1977).

[22]S. K. Chan and V. Heine, J. Phys. F 3, 795 (1973).

[23]J. A. Holy, Miles V. Klein, W. L. McMillan, and S. F. Meyer, Phys. Rev. Lett. 37, 1195 (1976). The samples used in this Raman study were from the same batch as we used in this paper.

[24]A. S. Barker, Jr., J. A. Ditzenberger, and F. J. DiSalvo, Phys. Rev. B 12, 2049 (1975).

[25]P. G. de Gennes and J. Friedel, J. Chem. Phys. Solids 4, 71 (1958).

[26]M. E. Fisher and J. S. Langer, Phys. Rev. Lett. 20, 665 (1968).

[27]Y. Suezaki and H. Mori, Prog. Theor. Phys. 41, 1177 (1969) and Phys. Lett. 28A, 70 (1969).

[28]As mentioned above, the resistivity at $2H$-$TaSe_2$ near T_0 bears a striking similarity to the resistivity of dysprosium near its antiferromagnetic phase transition. Dysprosium is an anisotropic rare-earth metal that develops a spiral antiferromagnetic phase below its Neel temperature ($T_N \simeq 180$ K). The superlattice wave vector Q in the spiral antiferromagnetic phase intersects the Fermi surface, and the periodic potential of the superlattice opens a gap in some region of this Fermi surface. The number of final states and density of electrons available for conduction are smaller below T_N than they are above T_N. Above the spiral antiferromagnetic phase transition, there are fluctuations into an antiferromagnetic state and the dominant wave vector of these fluctuations is Q. These fluctuations interact and scatter the electrons in the magnetic material via the spin-spin coupling. Since the wave vector of the spin fluctuation is large, it can change the momentum of the electron by a large amount, and hence is very effective at scattering electrons out of the forward direction. An increase in fluctuations of large wave vector, then, increases the back scattering and the resistivity. The population of fluctuations of a given wave vector in the magnetic case is related to the spin-spin correlation function. The resistivity, then, is also related to this population of fluctuations and is in fact dominated by the behavior of the spin-spin correlation function for temperatures near T_N. This correlation function for fluctuations of wave vector Q diverges at this temperature (see Ref. 17).

[29]P. M. Horn and D. Guidotti, Phys. Rev. B 16; 491 (1977).

[30]W. L. McMillan, Phys. Rev. B 12, 1187 (1975).

[31]D. E. Moncton, F. J. DiSalvo, J. D. Axe, L. J. Shaw, and B. R. Patton, Phys. Rev. B 14, 3432 (1976).

[32]M. E. Fisher and R. J. Buford, Phys. Rev. 156, 583 (1967).

[33]T. Kasuya and A. Kondo, Solid State Commun. 14, 253 (1974).